



**HAL**  
open science

## Additional risk in extreme precipitation in China from 1.5 °C to 2.0 °C global warming levels

Wei Li, Zhihong Jiang, Xuebin Zhang, Laurent Li, Ying Sun

► **To cite this version:**

Wei Li, Zhihong Jiang, Xuebin Zhang, Laurent Li, Ying Sun. Additional risk in extreme precipitation in China from 1.5 °C to 2.0 °C global warming levels. *Science Bulletin*, 2018, 63 (4), pp.228-234. 10.1016/j.scib.2017.12.021 . hal-02414647

**HAL Id: hal-02414647**

**<https://hal.science/hal-02414647>**

Submitted on 18 Dec 2019

**HAL** is a multi-disciplinary open access archive for the deposit and dissemination of scientific research documents, whether they are published or not. The documents may come from teaching and research institutions in France or abroad, or from public or private research centers.

L'archive ouverte pluridisciplinaire **HAL**, est destinée au dépôt et à la diffusion de documents scientifiques de niveau recherche, publiés ou non, émanant des établissements d'enseignement et de recherche français ou étrangers, des laboratoires publics ou privés.

1 **Additional risk in extreme precipitation in China from 1.5°C to 2.0°C**  
2 **global warming levels**

3  
4 **Wei Li**

5 Key Laboratory of Meteorological Disaster of Ministry of Education, Collaborative Innovation  
6 Center on Forecast and Evaluation of Meteorological Disaster, Nanjing University of  
7 Information Science and Technology, Nanjing, China

8  
9 **Zhihong Jiang\***

10 Joint International Research Laboratory of Climate and Environment Change, Collaborative  
11 Innovation Center on Forecast and Evaluation of Meteorological Disaster, Nanjing University  
12 of Information Science and Technology, Nanjing, China

13  
14 **Xuebin Zhang**

15 Climate Research Division, Environment and Climate Change Canada, Toronto, Ontario M3H  
16 5T4, Canada

17  
18 **Laurent Li**

19 Laboratoire de Météorologie Dynamique, CNRS, Sorbonne Universités,  
20 UPMC Université Paris 06, Paris, France

21  
22 **Ying Sun**

23 National Climate Center, Laboratory for Climate Studies, China Meteorological  
24 Administration, Beijing 100812, China

25  
26  
27  
28  
29  
30  
31  
32  
33  
34  
35  
36  
37  
38  

---

\* Corresponding Author: Zhihong Jiang, Key Laboratory of Meteorological Disaster of Ministry of Education, Collaborative Innovation Center on Forecast and Evaluation of Meteorological Disasters, Nanjing University of Information Science & Technology, Nanjing, 210044, China  
E-mail: zhjiang@nuist.edu.cn

39

## 40 **Abstracts**

41 To avoid dangerous climate change impact, the Paris Agreement sets out two ambitious  
42 goals: to limit the global warming to be well below 2 °C and to pursue effort for the  
43 global warming to be below 1.5 °C above the pre-industrial level. As climate change  
44 risks may be region-dependent, changes in magnitude and probability of extreme  
45 precipitation over China are investigated under those two global warming levels based  
46 on simulations from the Coupled Model Inter-Comparison Projects Phase 5. The focus  
47 is on the added changes due to the additional half a degree warming from 1.5 °C to 2 °C.  
48 Results show that regional average changes in the magnitude do not depend on the  
49 return periods with a relative increase around 7% and 11% at the 1.5 °C and 2 °C global  
50 warming levels, respectively. The additional half a degree global warming adds an  
51 additional increase in the magnitude by nearly 4%. The regional average changes in  
52 term of occurrence probabilities show dependence on the return periods, with rarer  
53 events (longer return periods) having larger increase of risk. For the 100-year historical  
54 event, the probability is projected to increase by a factor of 1.6 and 2.4 at the 1.5 °C and  
55 2 °C global warming levels, respectively. The projected changes in extreme  
56 precipitation are independent of the RCP scenarios.

57

58 Key words: 1.5°C and 2°C global warming, Extreme precipitation, China

59

60

61

62

63

64

65

66

67

68

69

70

71

72

73

## 74 **1. Introduction**

75 A global-scale warming has been dominating the Earth climate since the  
76 beginning of the industrial era. But to different magnitudes of temperature increase, the  
77 corresponding climate changes would exert different impacts on the global natural  
78 ecosystems and human societies. The question that what level of global warming is  
79 regarded as a dangerous warming threshold has been widely debated. The current  
80 international agreement about avoiding dangerous climate change impact was made  
81 under the United Nations Framework Convention on Climate Change (UNFCCC) at  
82 the 21st Conference of Parties (COP 21) in Paris. The agreement including two global  
83 warming targets: “holding the increase in the global average temperature to be well  
84 below 2 °C above pre-industrial and to pursue effort to limit the temperature increase to  
85 1.5 °C.” It is based on the hypothesis that maintaining the global warming below 1.5 °C  
86 would reduce the risks caused by climate change [1]. Meanwhile, UNFCCC invited the  
87 IPCC to elaborate a special report on the issue, which should be a comprehensive  
88 synthesis of the relevant scientific literature [2], [3], [4], [5], [6], [7]. The global mean  
89 warming is just an emblematic indicator, and vulnerability to global warming may vary  
90 from region to region and exhibit notable spatial inhomogeneity [3]. Therefore a  
91 differentiation of risks caused by climate change between 1.5 °C and 2 °C global  
92 warming levels is particularly important for highly sensitive regions [6]. China, a  
93 country with fragile ecological environment due to the fact that it has a prominent  
94 monsoon climate and has complex topography, is identified as a vulnerable region to  
95 global warming [8]. Floods after extreme precipitation cause considerable economic  
96 losses and serious damage to property. Therefore, it is necessary to rigorously assess  
97 physical and statistical characteristics of regional extreme precipitations when the  
98 global temperature increases by 1.5 °C and 2.0 °C relative to pre-industrial.

99

100 Global climate models are primary tools for investigating possible future change  
101 in climate extremes [9], [10], [11]. The Coupled Model Intercomparison Project Phase  
102 5 (CMIP5) of the World Climate Research Programme incorporates more physical

103 processes and higher resolution models than its previous phases [12]. Many results  
104 indicated that CMIP5 models can well reproduce the observed extreme precipitation at  
105 continental scale [13], [14] and regional scale [15], [16]. Climate responses to different  
106 global warming levels over China have been investigated in several recent studies using  
107 CMIP5. They mainly focus on the 2 °C warming target, including the timing of  
108 occurrence and the factors responsible for the timing uncertainties among models [17],  
109 [18]. This needs to investigate whether the expected changes exceed the natural internal  
110 variability [19], [20]. There are also researches investigating the extreme climate  
111 change with different warming targets (e.g. 2 °C, 3 °C, 4 °C) [21], [22], [23]. Recently,  
112 a few studies are reported on the climate change under 1.5 °C warming and the  
113 difference from 2 °C warming [24], [25]. However, limited attention has been paid to  
114 investigating extreme precipitation changes in term of magnitude and probability under  
115 1.5 °C and 2 °C warming levels.

116

117 This study uses statistical method to investigate two questions: How extreme  
118 precipitation may change under 1.5 °C and 2 °C global warming levels over China and  
119 how much is the influence of the extra half degree? Such questions are critical ones and  
120 should be addressed in an appropriate way. They are not only relevant to risk  
121 assessment and adaptation measures, but also useful to rationalize future international  
122 negotiations on climate change issues.

## 123 **2. Data and Methods**

### 124 2.1 Data

125 We use the daily precipitation datasets extracted from CMIP5 models in their  
126 historical experiments (1850–2005) with natural and anthropogenic forcing, and  
127 future simulations (2006–2100) with the Representative Concentration Pathway (RCP)  
128 scenarios [26]. In this study, we make relevant diagnostics on extreme precipitations  
129 under RCP4.5 and RCP8.5 scenarios. The reason for selecting those two scenarios is  
130 that RCP8.5 is mostly close to the observed emissions pathway, whereas RCP4.5  
131 represents a consideration of mitigation. The first realization from each model is

132 selected in order to treat all models equally. We select 1986–2005 as the reference  
133 period for assessment of future changes under the two warming targets.

134

135 Monthly surface air temperatures in both historical experiment and RCP  
136 scenarios are used to study the timing for the global mean temperature to reach the  
137 two warming targets for each model. Given that the observed global temperature in  
138 the reference period is 0.6 °C warmer than the pre-industrial level [27], the 1.5 °C and  
139 2 °C warming targets relative to pre-industrial imply warming of 0.9 °C and 1.4 °C  
140 relative to the reference period, respectively. We first calculate the average global  
141 temperature anomalies from 2006 to 2100 relative to the reference period by using the  
142 area-weighted scheme which takes into account the variation of grid box areas with  
143 latitude for individual models. The anomaly time series are then divided into a few  
144 20-year time slices to find the right period when the 0.9 °C and 1.4 °C warming  
145 thresholds occur for each model separately. The CMIP5 models used in this article  
146 and their timing to reach the two warming targets under RCPs scenarios are shown in  
147 Table 1.

148 There is a large difference among models when 1.5 °C and 2 °C warming targets  
149 are reached. For RCP4.5, the 20-year period of 1.5 °C warming ranges from [2013,  
150 2032] for BNU-ESM to [2046, 2065] for GFDL-ESM2G. For the 2 °C warming level,  
151 the 20-year period ranges from [2029, 2048] (HadGEM2-ES, MIROC-ESM and  
152 MIROC-EMS-CHEM) to [2064, 2083] (MRI-CGCM3). When the multi-model  
153 ensemble is examined, time reaching the two warming targets under RCP8.5 is earlier  
154 than under RCP4.5. Global warming reaches 1.5 °C under RCP4.5 and RCP8.5 at  
155 [2021, 2040] and [2016, 2035] respectively. The 2 °C warming is projected to be  
156 reached at [2041, 2060] for RCP4.5 and [2031, 2050] for RCP8.5. These results are  
157 consistent with former researches [6, 7, 18].

## 158 2.2 Methodology

159 Return value of annual daily precipitation is a widely used metric to measure the  
160 magnitude of extreme events [28], [29]. Also, return value is commonly used for a wide

161 range of applications on engineering planning, for instance, in the decision of  
 162 hydrologic design, water management structure, dams, and bridges. The return value  
 163 for a particular return period  $\tau$  is the threshold likely to be exceeded in a year with  
 164 probability  $1/\tau$ . Higher  $\tau$  means more intense and rarer extreme events. To estimate the  
 165 return value, annual maximum (AM) approach is used to select sample sequences from  
 166 daily data at every grid point to be fitted by generalized extreme value (GEV)  
 167 distribution. GEV distribution has been found suitable as a fit to the tails of the  
 168 distribution for precipitation. GEV distribution is also a generally reasonable  
 169 approximation for the distribution of annual extremes in most CMIP5 models [14].

170 The cumulative distribution function,  $G(z)$ , is given by (Coles, 2001) [30]:

$$171 \quad G(z) = \exp \left\{ - \left[ \xi \left( \frac{z - \mu}{\sigma} \right) \right]^{-1/\xi} \right\}, 1 + \xi \left( \frac{z - \mu}{\sigma} \right) > 0$$

172 where  $\mu$ ,  $\sigma$  and  $\xi$  are location, scale and shape parameters, respectively. These three  
 173 parameters are estimated by the method of “L-moments”, which is more efficient and  
 174 generates less uncertainty compared to other methods to estimate parameters over a  
 175 small sample size [31]. Having estimated the parameters, return value,  $z_p$ ,  
 176 corresponding to the return period  $\tau = 1/p$ , can be determined after inverting the  
 177 GEV cumulative distribution function.

$$178 \quad z_p = \mu - \frac{\sigma}{\xi} \left[ 1 - \{-\log(1 - p)\}^{-\xi} \right], \xi \neq 0$$

179 where  $p$  is an exceedance probability. In addition, we can examine the probability  
 180 change of extreme precipitation by using probability ratio (PR), a metric  
 181 characterizing the factor by which probability of an event has changed [32, 33],  
 182 defined as  $PR = P_1/P_0$ , where  $P_0$  denotes the probability of  $\tau_0$ -year return value  
 183 during the reference period and  $P_1$  during 1.5°C or 2°C warming climate, expressed  
 184 as a future return period  $\tau_1 = 1/P_1$ ,  $P_1/P_0 = \tau_0/\tau_1$ . If  $PR > 1$ , probability of reference  
 185 period events would increase at 1.5°C or 2°C warming environment.

186 Three different return periods events (20-, 50-, and 100-year) of annual maxima  
 187 precipitation for the reference period (1986-2005) and the 20-year slices when global  
 188 warming reaches the two warming levels for individual models are derived from the

189 fitted GEV. PR of historical (for three return periods) events at the two levels of  
 190 warming climate can also be determined. Those two statistical values from different  
 191 models are interpolated onto a common  $1^\circ \times 1^\circ$  latitude-longitude grid with a bilinear  
 192 interpolation scheme.

193 Additionally, GEV distribution allows the incorporation of covariates in  
 194 parameters to estimate the dependence of extreme precipitation change on global  
 195 mean temperature anomaly, which can provide more information about extreme  
 196 precipitation change with further global warming. Here, the location and scale  
 197 parameters are assumed to be function of global mean temperature anomaly and the  
 198 shape parameter is kept constant. Because the scale parameter must be positive  
 199 everywhere, it is often modeled using a log link function, such that:

$$200 \quad \mu(t) = \mu_0 + \mu_1 y(t)$$

$$201 \quad \ln \sigma(t) = \sigma_0 + \sigma_1 y(t)$$

202 where  $y(t)$  is the global mean temperature anomaly from 1961 to 2100 relative to the  
 203 pre-industrial in year  $t$ .  $\mu_0, \mu_1, \sigma_0, \sigma_1$  are regression parameters to be estimated. The  
 204 cumulative distribution function,  $G(z_t)$  can be expressed as

$$205 \quad G(z_t) = \exp \left\{ - \left[ \xi \left( \frac{z_t - \mu(t)}{\sigma(t)} \right) \right]^{-1/\xi} \right\}, 1 + \xi \left( \frac{z_t - \mu(t)}{\sigma(t)} \right) > 0$$

206 Return value  $Z_{p_t}$  is defined as

$$207 \quad Z_{p_t} = \mu_t - \frac{\sigma_t}{\xi} [1 - \{-\log(1 - p)\}^{-\xi}], \xi \neq 0$$

208 There are five parameters ( $\mu_0, \mu_1, \sigma_0, \sigma_1, \xi$ ) in nonstationary GEV distribution. Those  
 209 five parameters are estimated by the method of maximum likelihood estimation (MLE)  
 210 [34]. An advantage of MLE is that it is efficient when the sample size is large and it is  
 211 particularly preferred in estimating parameters for nonstationary data. Here,  
 212 nonstationary GEV is fitted to time series of annual maxima precipitation for the  
 213 period 1961-2100 for individual models. The magnitude and probability change  
 214 relative to historical at given global warming target can be derived from fitted  
 215 nonstationary GEV.

### 216 3. Results

### 217 3.1 Changes in the magnitude of extreme precipitation

218 Changes in magnitude of extreme precipitation relative to the reference period at  
219 the two warming levels under RCP4.5 and RCP8.5 were analyzed with the annual  
220 precipitation maxima from individual CMIP5 models fitted to stationary GEV (Fig. 1).  
221 Regionally averaged, the relative changes of return periods in the multi-model  
222 ensemble mean (MME) (black point) under RCP4.5 are close to RCP8.5 scenario.  
223 This indicates that changes in magnitude of extreme precipitation are not very much  
224 independent on emission scenarios when the global warming level reaches a given  
225 warming target.

226 It can be seen that there is little difference among return periods under same  
227 warming conditions. The amplitude is projected to increase by about 7% and nearly  
228 11% when global warming reaches to 1.5 °C and 2 °C, respectively. Extra half a  
229 degree warming makes the intensity to increase by nearly 4%. If we use the dispersion  
230 of models to represent the projection uncertainties, we can see that the projection  
231 uncertainties vary among return periods, with larger uncertainty at higher return  
232 period. Meanwhile, uncertainties at higher warming level are larger than that at lower  
233 warming level.

234

235 We examine now the spatial distribution of intensity difference between the  
236 1.5 °C and 2 °C worlds for RCP4.5 and RCP8.5 scenarios (Fig. 1S). As expected, the  
237 changes in 20-, 50-, and 100-year return value show a very similar spatial distribution.  
238 Compared to 1.5 °C warming, the magnitude of extreme precipitation is projected to  
239 increase under 2 °C warming across most of the region for both scenarios. In many  
240 regions where the magnitude increases, especially for regions with large increase, the  
241 consistency among models is high. Areas where large increases are projected to occur  
242 show a dependence on scenarios. Areas with an increase larger than 5% are  
243 concentrated in most of Western China and Southeastern China for RCP4.5, while for  
244 RCP8.5, such areas of increase are mainly in Western China and North China, but not  
245 in Southeastern China. These results are generally in agreement with previous studies  
246 showing that a larger magnitude of extreme precipitation can be found in those

247 regions under the context of global warming [35], [11], [36]. The difference in  
248 intensity change between RCP4.5 and RCP8.5 also indicates that the finer change of  
249 extreme precipitation at regional scale from global models still have large  
250 uncertainties.

251

252 The magnitude change of extreme precipitation with future global warming can  
253 also be seen if the nonstationary GEV scheme is applied to the transient simulations.  
254 Fig. 2 displays the regional average changes (which is relative to reference period) of  
255 the three return periods as a function of global mean temperature anomaly (which is  
256 relative to pre-industrial) simulated by CMIP5 models for RCP4.5 and RCP8.5  
257 scenarios. It is noted that the global warming in the multi model ensemble mean do  
258 not exceed 3 °C relative to pre-industrial for RCP4.5 and 5 °C for RCP8.5 scenario, so  
259 we only show the relationship within the period where global warming may reach.  
260 Results of non-stationary calculation show very similar results as in the stationary  
261 calculation. This is particularly true for the change of magnitude in MME and  
262 uncertainties among models when warming reaches 1.5 °C and 2 °C. The  
263 nonstationary results show that the magnitude increases in MME nonlinearly with  
264 future warming. For example, the magnitude is expected to increase by nearly 8%  
265 when global mean temperature warms from 1 °C to 2 °C, while the increase is about 5%  
266 when the global mean temperature increases from 3 °C to 4 °C under RCP8.5.

### 267 3.2 Change in the probability of extreme precipitation

268 The probability change of historical extreme events at two warming levels is  
269 analyzed in this section. The regional average PR of historical events for the three  
270 return periods is illustrated in Fig. 3 for the two warming levels. As expected, the  
271 MME results show little distinction between RCP4.5 and RCP8.5 scenarios.  
272 Generally speaking, the probabilities of historical extreme events are projected to  
273 increase in response to the global warming. PR increases most strongly for the longest  
274 return periods, especially at higher warming level, which implies that the most intense  
275 and rarest extreme precipitation events have largest increase in the risk. Taken 2 °C

276 warming as an example, the probability of historical 20-yr events increases by a factor  
277 of 1.9, however, for historical 100-year events, the probability increases by a factor of  
278 2.4.

279 Probability of historical 100-year events increases by about a factor of 1.6 under  
280 1.5 °C warming and 2.4 under 2 °C warming climate. This implies that regional  
281 average event expected once every 100 years in historical period is expected to occur  
282 about every 62 and 42 years under 1.5 °C and 2 °C warming climate, respectively. The  
283 100-year event of 1.5 °C warming is almost 1.4 times more likely to occur at 2 °C  
284 warming.

285

286 Similar to the relative changes of magnitude in extreme precipitation, the  
287 inter-model variation of PR is significant across the three return periods for a given  
288 warming level, with larger inter-model spreading at higher return periods. For  
289 example, PR of a historical 20-year event ranges from 1.4 to 2.8 under 2 °C warming  
290 level, but for 100-year events, PR ranges from 1.6 to 4.2. Furthermore, the  
291 inter-model spreading of PR under higher warming climate is also larger. PR of a  
292 historical 100-year event at 1.5 °C and 2 °C warming levels ranges from 1.0 to 2.6 and  
293 1.6 to 4.2, respectively.

294

295 The spatial distribution of PR variation between 1.5 °C warming and 2 °C  
296 warming is also researched (Fig. 2S). We show the cases for 20-, 50-, and 100-year  
297 events and for the two scenarios. The risk of extreme events at 1.5 °C warming level  
298 is projected to increase almost everywhere at 2 °C warming over China for both RCP  
299 scenarios. PR of 20-, 50-, and 100-year events shows a very similar spatial  
300 distribution, although it varies depending on the return periods with higher return  
301 periods associated to larger PR. Areas where PR is larger than 2.0 show a future  
302 strengthening and extension with increasing of return periods. Those regions also  
303 depend on scenarios. The largest PR for RCP4.5 is projected to occur over large zones  
304 in western China, especially around the Tibetan Plateau. For RCP8.5, the largest PR  
305 occurs over western China and the Yangtze River. Events that would be attained once

306 every 50 and 100 years in 1.5 °C warming climate will be 2 times more likely to occur  
307 at 2 °C warming climate in those regions. Meanwhile, regions with large increase of  
308 probability also exhibit a relative high models consistency.

309

310 In order to study how the probability changes with future global warming, we  
311 examine the probability change of historical extreme events with increases of global  
312 mean temperature by using the non-stationary GEV distribution. Fig. 4 displays the  
313 regional average PR of historical extreme events at a given warming levels relative to  
314 pre-industrial conditions in CMIP5 models for RCP4.5 and RCP8.5 scenarios. Also,  
315 results of PR exhibit no difference between the stationary and nonstationary schemes  
316 for MME and inter-model spread. However, with further warming, the PR of  
317 historical events in MME increases nonlinearly, especially for the very rare events.  
318 The probability of historical 100-year events increases 2 times when global warming  
319 increases from 4 °C to 5 °C. However, when global warming increases from 1 °C to  
320 2 °C, the probability of historical 100-year events only increases 1 time. It is also  
321 noted that the uncertainties among models would be larger at higher warming. For  
322 instance, the range of models for PR of 100-year historical events at 4 °C warming is  
323 nearly 13 times higher than that at 1 °C warming.

#### 324 **4. Summary**

325 In this study, future changes in magnitude and probability of extreme  
326 precipitation are investigated at global warming levels of 1.5°C and 2°C above  
327 pre-industrial. The magnitude and probability of extreme precipitation are described  
328 by the return values corresponding to three return periods and probability risk,  
329 respectively. Major findings are summarized as follows.

330 (1) Changes of extreme precipitation from MME show less dependences on the  
331 emission scenarios of RCP4.5 and RCP8.5 when global warming reaches two  
332 warming levels.

333 (2) Relative changes in the magnitude exhibit little difference for different return  
334 periods under the same warming threshold. Magnitude is projected to increase by

335 about 7% for 1.5°C warming and 11% for 2°C warming relative to reference  
336 period. The additional half a degree warming makes the extreme precipitation to  
337 increase by 4%.

338 (3) Probabilities of a given change depend on the return periods. The rarest events  
339 (the longest return period) have largest increase in the risk for a given warming  
340 level. For historical 100-year events, their occurrence probability increases by 1.6  
341 times at 1.5°C warming, whereas at a 2°C warming, the increase is about 2.4 times.  
342 The 100-year event of 1.5°C is 1.4 times more likely to occur at 2°C warming  
343 condition.

344 (4) Uncertainties among models for magnitude and probability of change increase  
345 with global warming and higher return period events exhibits larger uncertainties.

346 Our research is one of the first studies targeting two global warming levels at 1.5°C  
347 and 2°C over China. For both of them, extreme precipitation shows stronger  
348 magnitude and higher probability. Changes are generally larger under 2°C global  
349 warming level compared to 1.5°C global warming. The additional half-degree  
350 warming does matter for eventual mitigation measures against extreme precipitation  
351 events. We should remind that global climate models are generally of low spatial  
352 resolution and they suffer imperfections for physical processes, which causes  
353 differences and uncertainties among models in projecting regional-scale climate  
354 changes. Some regional climate modelling efforts in East Asia show that a higher  
355 resolution may give a more accurate regional climate [37-39]. Therefore, more  
356 experiments with higher-resolution regional climate models are needed to address this  
357 issue of regional climate change.

358

## 359 **Acknowledgments**

360 We acknowledge the World Climate Research Programme's Working Group on  
361 Couple modelling and the modeling groups listed in Table S1 of this paper for making  
362 their simulations available for analysis, the PCMDI for collecting and archiving the  
363 CMIP5 model output (<http://pcmdi9.llnl.gov>.) This work is supported by the National  
364 Key R&D Program of China (Grant 2017YFA0603804), the State Key Program of

365 National Natural Science Foundation of China (41230528), and  
366 the China Scholarship Council (CSC) under the State Scholarship Fund. L. Li was  
367 partly supported by the French ANR Project China-Trend-Stream.

368

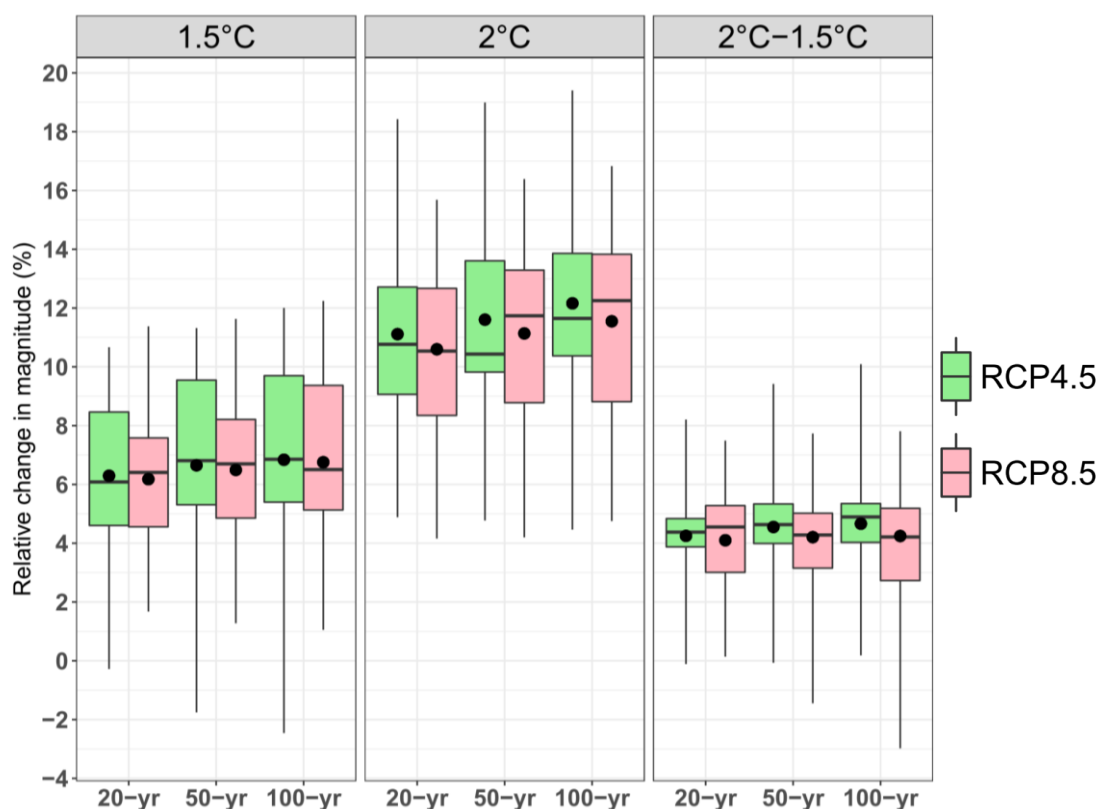
## 369 Reference

- 370 1. UNFCCC: Decision 1/CP.21, The Paris Agreement. 2015.
- 371 2. Donnelly C, Greuell W, Andersson J, et al. Impacts of climate change on European  
372 hydrology at 1.5, 2 and 3 degrees mean global warming above preindustrial level.  
373 *Clim Change*, 2017; 143: 1-14.
- 374 3. Schleussner, C, Lissner, T, Fischer E, et al. Differential climate impacts for  
375 policy-relevant limits to global warming: the case of 1.5°C and 2°C, *Earth Syst Dyn*,  
376 2016; 7: 327–351.
- 377 4. King A D, Karoly, D J, Henley, B J. Australian climate extremes at 1.5°C and 2°C  
378 of global warming. *Nat Clim Change*, 2017; 7(6): 412-416.
- 379 5. Schaeffer M, Hare W, Rahmstorf S, Vermeer M. Long-term sea-level rise implied  
380 by 1.5°C and 2°C warming levels. *Nat Clim Change*, 2012; 2(12):867.
- 381 6. Seneviratne S I, Donat M G, Pitman A J, et al. Allowable CO2 emissions based on  
382 regional and impact-related climate targets, *Nature*, 2016; 1870, 1-7.
- 383 7. Karmalkar A V, Bradley R S. Consequences of Global Warming of 1.5°C and 2°C  
384 for Regional Temperature and Precipitation Changes in the Contiguous United  
385 States. *PloS one*, 2017; 12(1): e0168697.
- 386 8. Huang, J., Liu, Y., Ma, L., and Su, F. Methodology for the assessment and classification of  
387 regional vulnerability to natural hazards in China: the application of a DEA model. *Natural*  
388 *hazards*, 2013; 65(1), 115-134.
- 389 9. Sillmann, J., Kharin, V. V., Zwiers, F. W., Zhang, X., and D. Bronaugh. Climate extremes  
390 indices in the CMIP5 multimodel ensemble: Part 2. Future climate projections, *J.*  
391 *Geophys. Res.-Atmos.*, 2013, 118(6), 2473-2493.
- 392 10. Knutti, R., and J. Sedláček .Robustness and uncertainties in the new CMIP5 climate  
393 model projections, *Nature Climate Change*, 2013; 3(4), 369-373.
- 394 11. Li, W., Jiang, Z., Xu, J., and L. Li, Extreme Precipitation Indices over China in CMIP5  
395 Models. Part II: Probabilistic Projection, *J. Climate*, 2016; 29(24), 8989-9004.
- 396 12. Taylor, K. E., Stouffer, R. J., & Meehl, G. A. (2012). An overview of CMIP5 and  
397 the experiment design. *Bulletin of the American Meteorological Society*, 93(4),  
398 485-498.
- 399 13. Sillmann, J., Kharin, V. V., Zhang, X., Zwiers, F. W., and Bronaugh, D. Climate extremes  
400 indices in the CMIP5 multimodel ensemble: Part 1. Model evaluation in the present  
401 climate. *Journal of Geophysical Research: Atmospheres*, 2013; 118(4), 1716-1733.
- 402 14. Kharin, V. V., Zwiers, F. W., Zhang, X., and Wehner, M. Changes in temperature and  
403 precipitation extremes in the CMIP5 ensemble. *Climatic change*, 2013; 119(2), 345-357.
- 404 15. Jiang, Z., Li, W., Xu, J., and Li, L. Extreme precipitation indices over China in CMIP5  
405 models. Part I: Model evaluation. *Journal of Climate*, 2015; 28(21), 8603-8619.

- 406 16. Ou, T., D. Chen, H. W. Linderholm, and J. H. Jeong. Evaluation of global climate models in  
407 simulating extreme precipitation in China. *Tellus*, 2013; 65A, 1393–1399,
- 408 17. Chen X, and Zhou T. Uncertainty in crossing time of 2°C warming threshold over  
409 China. *Chin Sci Bull*, 2016; 61(18): 1451-1459.
- 410 18. Zhang L, Ding Y, Wu T, Xin X, Zhang Y, Xu Y. The 21st century annual mean  
411 surface air temperature change and the 2°C warming threshold over the globe and  
412 China as projected by the CMIP5 models. *Acta Meteorol Sin*, 2013; 71(6):  
413 1047-1060
- 414 19. Jiang D B, Yue S, and Lang X. Timing and associated climate change of a 2°C  
415 global warming. *Int J Climatol*, 2016; 36(14): 4512-4522.
- 416 20. Sui Y, Lang X, Jiang D. Temperature and precipitation signals over China with a  
417 2°C global warming. *Clim Res*, 2015; 64(3):227-242.
- 418 21. Jiang D B, Zhang Y, and Sun J. Ensemble projection of 1–3°C warming in  
419 China. *Chin Sci Bull*, 2009; 54(18): 3326-3334.
- 420 22. Guo X, Huang J, Luo Y, et al. Projection of precipitation extremes for eight global  
421 warming targets by 17 CMIP5 models. *Nat Hazards*, 2016; 84(3): 2299-2319.
- 422 23. Tian, D., W. Dong, H. Zhang, et al. Future changes in coverage of 1.5 °C and 2 °C  
423 warming thresholds. *Sci Bull*, 62 (2017), pp. 1455-1463
- 424 24. Chen J, Gao C, Zeng X, et al. Assessing changes of river discharge under global  
425 warming of 1.5° C and 2° C in the upper reaches of the Yangtze River Basin:  
426 Approach by using multiple-GCMs and hydrological models. *Quat Int*, 2017; 435:  
427 63-73.
- 428 25. HU, T., SUN, Y., & ZHANG, X. (2017). Temperature and precipitation projection at 1.5 and  
429 2° C increase in global mean temperature. *Chinese Science Bulletin*, 62(26), 3098-3111.
- 430 26. Moss, R. H., Edmonds, J. A., Hibbard, K. A., et al. The next generation of scenarios  
431 for climate change research and assessment. *Nature*, 2010; 463(7282), 747-756.
- 432 27. Harmann D L, Klevin Tank A M G, Rusticucci M, et al. Observations:  
433 Atmosphere and Surface. In: Stocker T F, Qin D H, Plattner G K, et al., eds.  
434 Climate Change 2013: The Physical Science Basis. Contribution of Working  
435 Group I to the Fifth Assessment Report of the Intergovernmental Panel on Climate  
436 Change. Cambridge: Cambridge University Press, 2013; 159-254
- 437 28. Zhang Y, Gao Z, Pan Z. Li D, et al. Spatiotemporal variability of extreme  
438 temperature frequency and amplitude in China. *Atmos Res*, 2017; 185: 131-141.
- 439 29. Kharin V V, Zwiers F W, Zhang X, et al. Changes in temperature and precipitation  
440 extremes in the IPCC ensemble of global coupled model simulations. *J Climate*,  
441 2007; 20(8): 1419-1444.
- 442 30. Coles S. An Introduction to Statistical Modeling of Extreme Values,  
443 Springer-Verlag, 2001; 208 pp.
- 444 31. Hosking J M R and James R W. Regional frequency analysis: an approach based on  
445 L-moments. Cambridge University Press, 2005.
- 446 32. Stott P A, Dáithí A S, and Myles R A. Human contribution to the European  
447 heatwave of 2003. *Nature*, 2004; 432(7017): 610-614.
- 448 33. Fischer E M and Knutti R. Anthropogenic contribution to global occurrence of  
449 heavy-precipitation and high-temperature extremes. *Nat Clim Change*, 2015; 5(6):

- 450           560-564.
- 451 34. Martins E S and Stedinger J R. Generalized Maximum Likelihood Pareto-Poisson  
452       estimators for partial duration series. *Water Resour Res*, 2001; 37(10): 2551-2557.
- 453 35. Chen H P. Projected change in extreme rainfall events in China by the end of the  
454       21st century using CMIP5 models. *Chin Sci Bull*, 2013; 58: 1462–1472
- 455 36. Wang L, Chen W. A CMIP5 multimodel projection of future temperature,  
456       precipitation, and climatological drought in China. *Int J Climatol*, 2014; 34(6):  
457       2059-2078.
- 458 37. Yang H, Jiang Z, and Li, L. Biases and improvements in three dynamical  
459       downscaling climate simulations over China, *Clim Dyn*, 2016; 47(9-10):  
460       3235-3251
- 461 38. Zou L, and Zhou, T. Future summer precipitation changes over CORDEX-East  
462       Asia domain downscaled by a regional ocean-atmosphere coupled model: A  
463       comparison to the stand-alone RCM, *J Geophys Res Atmos*, 2016; 121(6):  
464       2691-2704.
- 465 39. Gao X J, Shi Y, Giorgi F. Comparison of convective parameterizations in RegCM4  
466       experiments with CLM as the land surface model over China. *Atmospheric and*  
467       *Oceanic Science Letters*, 2016; 9(4), 246–254.
- 468
- 469

470



471

472 **Fig.1** Boxplots of the regional average relative change (relative to 1986-2005  
 473 reference period, units: %) in the 20-, 50-, 100-year return values for 1.5°C (left panel)  
 474 and 2°C (middle panel) warming level, as well as the difference between the two  
 475 warming levels (right panel) among models under RCP4.5 and RCP8.5 scenario. The  
 476 upper and lower limits of the box indicate the 75<sup>th</sup> and 25<sup>th</sup> percentile value among  
 477 models; the horizontal line in the box indicates the multi-model ensemble median and  
 478 the whiskers show the range of models. MME is represented by black points.

479

480

481

482

483

484

485

486

487

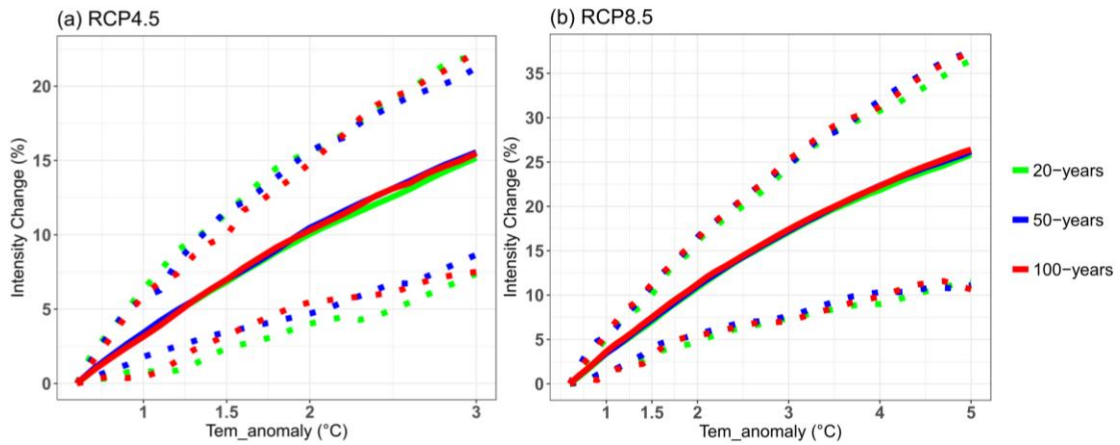
488

489

490

491

492



493

494 **Fig.2** The relationship between relative change (%) in regional average 20- (green),  
495 50- (blue), and 100-year (red) return values (relative to reference period) and global  
496 mean temperature anomaly (relative to pre-industrial) in CMIP5 models for RCP4.5  
497 (a) and RCP8.5 (b). Solid lines indicate the MME and the dotted lines are the  
498 uncertainties range.

499

500

501

502

503

504

505

506

507

508

509

510

511

512

513

514

515

516

517

518

519

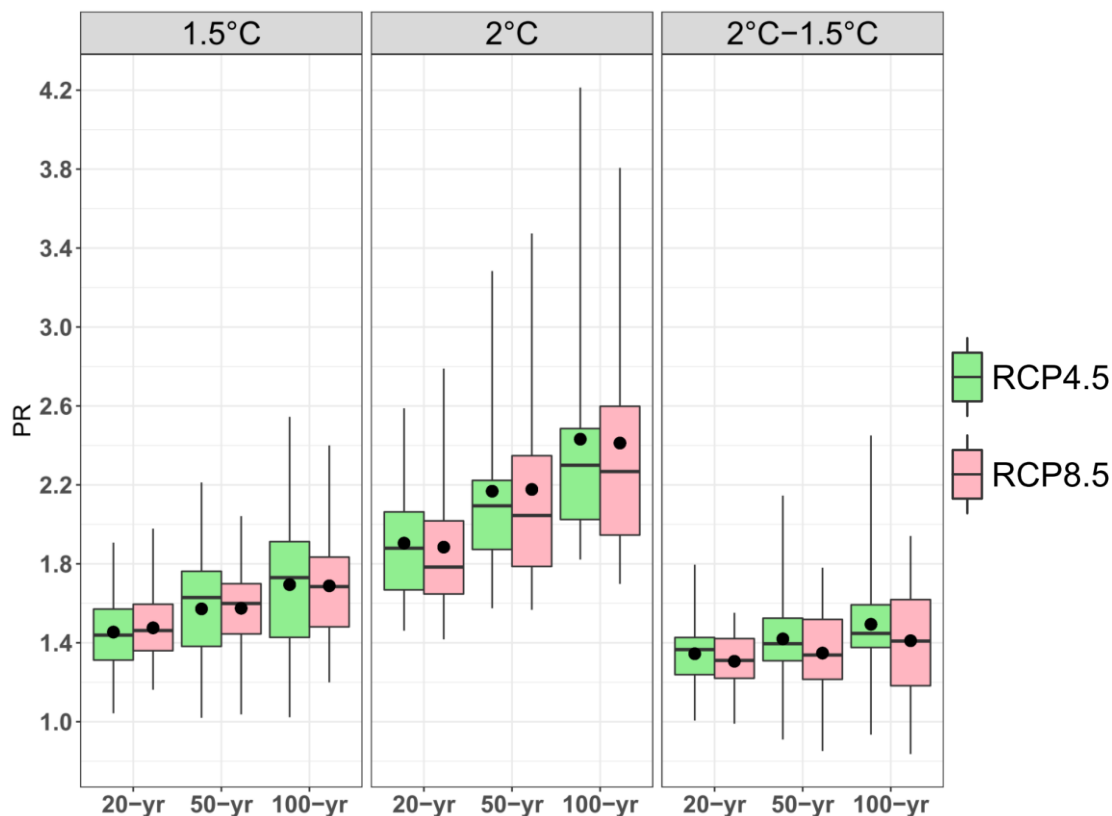
520

521

522

523

524



525

526 **Fig.3** Boxplots of PR for the historical 20-, 50-, 100-year return values in 1.5°C (left  
 527 panel) and 2°C (middle panel) warming conditions among models, as well as PR of  
 528 1.5°C warming events in 2°C warming conditions (right panel) under RCP4.5 and  
 529 RCP8.5 scenarios. The upper and lower limits of the box indicate the 75th and 25th  
 530 percentile value among models; the horizontal line in the box indicates the  
 531 multi-model ensemble median and the whiskers show the range of models. MME is  
 532 represented by black points.

533

534

535

536

537

538

539

540

541

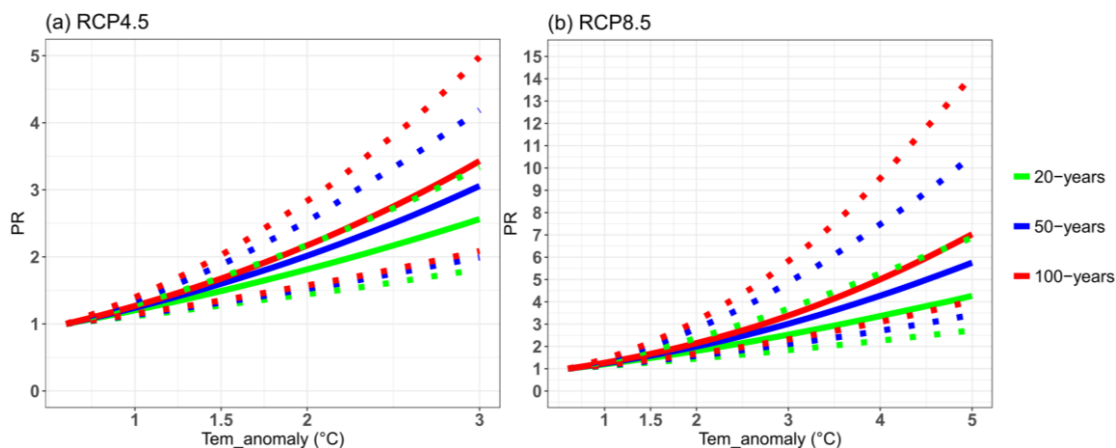
542

543

544

545

546  
547  
548  
549



550

551 **Fig. 4** The relationship between PR of historical 20- (green), 50- (blue), and 100-year  
552 (red) return values and global mean temperature anomaly (relative to pre-industrial)  
553 for RCP4.5 and RCP8.5. Solid lines indicate the MME and the two dotted lines  
554 represent the uncertainties range.

555  
556  
557  
558  
559  
560  
561  
562  
563  
564  
565  
566  
567  
568  
569  
570  
571  
572  
573  
574  
575  
576  
577

578

579

580

581

582 **Table 1** The CMIP5 models used in this article, together with their atmospheric  
 583 model's resolution and the 20-year time slices when global warming reaches 1.5°C  
 584 and 2°C relative to pre-industrial period under RCP4.5 and RCP8.5 scenarios.

Model name	Atmospheric resolution	RCP4.5		RCP8.5	
		1.5°C	2 °C	1.5°C	2 °C
ACCESS1.0	~1.9°×1.25°, L38	[2018,2037]	[2041,2060]	[2016,2035]	[2029,2048]
ACCESS1.3	~1.9°×1.25°, L38	[2020,2039]	[2039,2058]	[2015,2034]	[2029,2048]
BCC-CSM1.1	~2.8°×~2.8°, L26	[2026,2045]	[2062,2081]	[2022,2041]	[2036,2055]
BCC-CSM1.1(m)	~1.1°×~1.1°, L26	[2020,2039]	[2063,2082]	[2015,2034]	[2034,2053]
BNU-ESM	~2.8°×~2.8°, L26	[2013,2032]	[2032,2051]	[2012,2031]	[2024,2043]
CanESM2	~2.8°×~2.8°, L35	[2014,2033]	[2028,2047]	[2009,2028]	[2022,2041]
CCSM4	1.25°×~0.9°, L26	[2025,2044]	[2052,2071]	[2015,2034]	[2032,2051]
CMCC-CM	0.75°×~0.75°, L31	[2024,2043]	[2041,2060]	[2028,2047]	[2040,2059]
CMCC-CMS	~1.9°×~1.9°, L95	[2022,2041]	[2039,2058]	[2017,2036]	[2029,2048]
CNRM-CM5	~1.4°×~1.4°, L31	[2029,2048]	[2051,2070]	[2022,2041]	[2036,2055]
HadGEM2-CC	~1.9°×1.25°, L40	[2017,2036]	[2033,2052]	[2008,2027]	[2022,2041]
IPSL-CM5A-LR	3.75°×~1.9°, L39	[2019,2038]	[2035,2054]	[2015,2034]	[2027,2046]
IPSL-CM5A-MR	2.5°×~1.25°, L39	[2015,2034]	[2036,2055]	[2014,2033]	[2027,2046]
MIROC5	~1.4°×~1.4°, L40	[2025,2044]	[2053,2072]	[2021,2040]	[2037,2056]
MIROC-ESM	~2.8°×~2.8°, L80	[2015,2034]	[2029,2048]	[2013,2032]	[2023,2042]
MIROC-ESM-CHEM	~2.8°×~2.8°, L80	[2014,2033]	[2029,2048]	[2010,2029]	[2022,2041]
MPI-ESM-LR	~1.9°×~1.9°, L47	[2024,2043]	[2055,2074]	[2019,2038]	[2034,2053]
MPI-ESM-MR	~1.9°×~1.9°, L95	[2027,2046]	[2048,2067]	[2022,2041]	[2036,2055]
MRI-CGCM3	~1.1°×~1.1°, L48	[2034,2053]	[2064,2083]	[2026,2045]	[2039,2058]
NorESM1-M	2.5°×~1.9°, L26	[2028,2047]	[2060,2079]	[2022,2041]	[2038,2057]

585

586